Geol. Mag. **153** (*1*), *2016, pp. 128–142.* © *Cambridge University Press 2015*
doi:10.1017/S0016756815000448

U–Pb geochronology of the Eocene Kærven intrusive complex, East Greenland: constraints on the Iceland hotspot track during the rift-to-drift transition

SIGURJÓN B. THÓRARINSSON*†‡, PAUL M. HOLM†, SEBASTIAN TAPPE§¶, LARRY M. HEAMAN¶ & NIELS-OLE PRÆGEL‖

*Nordic Volcanological Center, Institute of Earth Sciences, University of Iceland, Askja, Sturlugata 7, IS-101 Reykjavik, Iceland
†Department of Geosciences and Natural Resource Management, University of Copenhagen, Øster Voldgade 10, DK-1350 København K, Denmark
§Department of Geology, University of Johannesburg, PO Box 524, Auckland Park 2006, Johannesburg, South Africa
¶Department of Earth and Atmospheric Sciences, University of Alberta, Edmonton, AB T6G 2E3, Canada
‖Copenhagen University Library, Nørre Allé 49, DK-2200 København K, Denmark

(*Received* 23 December 2014; *accepted* 27 May 2015; *first published online* 3 July 2015)

Abstract – Several major tholeiitic (e.g. the Skaergaard intrusion) and alkaline (e.g. the Kangerlussuaq Syenite) intrusive complexes of the North Atlantic Large Igneous Province are exposed along the Kangerlussuaq Fjord in East Greenland. The Kærven Complex forms a satellite intrusion to the Kangerlussuaq Syenite and includes early tholeiitic gabbros and a series of cross-cutting alkaline intrusions ranging from monzonite to alkali granite. The alkaline intrusions cut the gabbros, and are cut by the outer nordmarkite zone of the Kangerlussuaq Syenite. This study presents the first U–Pb zircon ages from the alkaline units of the Kærven Complex. Fourteen multi-grain zircon fractions have been analysed by thermal ionization mass spectrometry (TIMS). Absolute age differences could not be resolved between the different units, suggesting a relatively rapid succession of intrusions between *c.* 53.5 and 53.3 Ma. Our compilation of precise radiometric age data shows that most of the alkaline magmatism in the Kangerlussuaq Fjord occurred prior to 50 Ma. Moreover, pre-50 Ma alkaline intrusions and lavas show a SSE-younging trend, which is interpreted as the track of the Iceland hotspot during the rift-to-drift transition of the North Atlantic.

Keywords: Kangerlussuaq, zircon, syenite, post-break-up, North Atlantic Igneous Province.

1. Introduction

Central East Greenland was the site of massive outpourings of tholeiitic flood basalt during the Early Palaeogene period as exemplified by the *c.* 7-km-thick Blosseville Kyst lava succession (Fig. 1) emplaced between 61 and 55 Ma (Storey, Duncan & Swisher, 2007). The extensive magmatism has generally been attributed to large degrees of mantle decompression melting, driven by both the impact of the Iceland mantle plume beneath the Greenland lithosphere and subsequent continental break-up and opening of the North Atlantic Ocean at 56–54 Ma (e.g. Saunders *et al.* 1997; Storey, Duncan & Tegner, 2007). Although the North Atlantic track of the hotspot is tightly constrained by the Greenland–Iceland Ridge, a *c.* 300-km-wide section of anomalously thick oceanic crust immediately seawards of the East Greenland rifted margin (Fig. 1), the path of the hotspot beneath Greenland and the timing of the track are still debated. Early models suggested that the mantle plume was centred directly under the ensuing rift during continental break-up (Brooks, 1973; White & McKenzie, 1989; Saunders *et al.* 1997). Plate-kinematic reconstructions, however, indicate that the plume axis was located under central Greenland during break-up and that the rifted margin first crossed the plume axis sometime after break-up (Duncan & Richards, 1991; Lawver & Müller, 1994; Torsvik *et al.* 2001). Bernstein *et al.* (1998) and Tegner *et al.* (1998) argue that abundant post-break-up tholeiitic and alkaline magmatism at 50–47 Ma records this crossing. The magmatism during this period appears to have been confined to a *c.* 600 km broad region along the East Greenland coast between 66° and 70°N, with the strongest geochemical plume signatures occurring in a *c.* 150-km-broad zone centred near the Kangerlussuaq Fjord (Fig. 1). This is in good agreement with the width of the Greenland–Iceland Ridge (Bernstein *et al.* 1998; Tegner *et al.* 1998).

The Kangerlussuaq Fjord is a major tectonic lineament that has been interpreted as the failed arm of a triple junction. Flood basalt volcanism and intrusion of dyke swarms, followed by active seafloor spreading, occurred in two arms parallel to the present-day coastline (Brooks, 1973; Burke & Dewey, 1973; Karson & Brooks, 1999). The third arm, now occupied

‡Author for correspondence: sith@ign.ku.dk

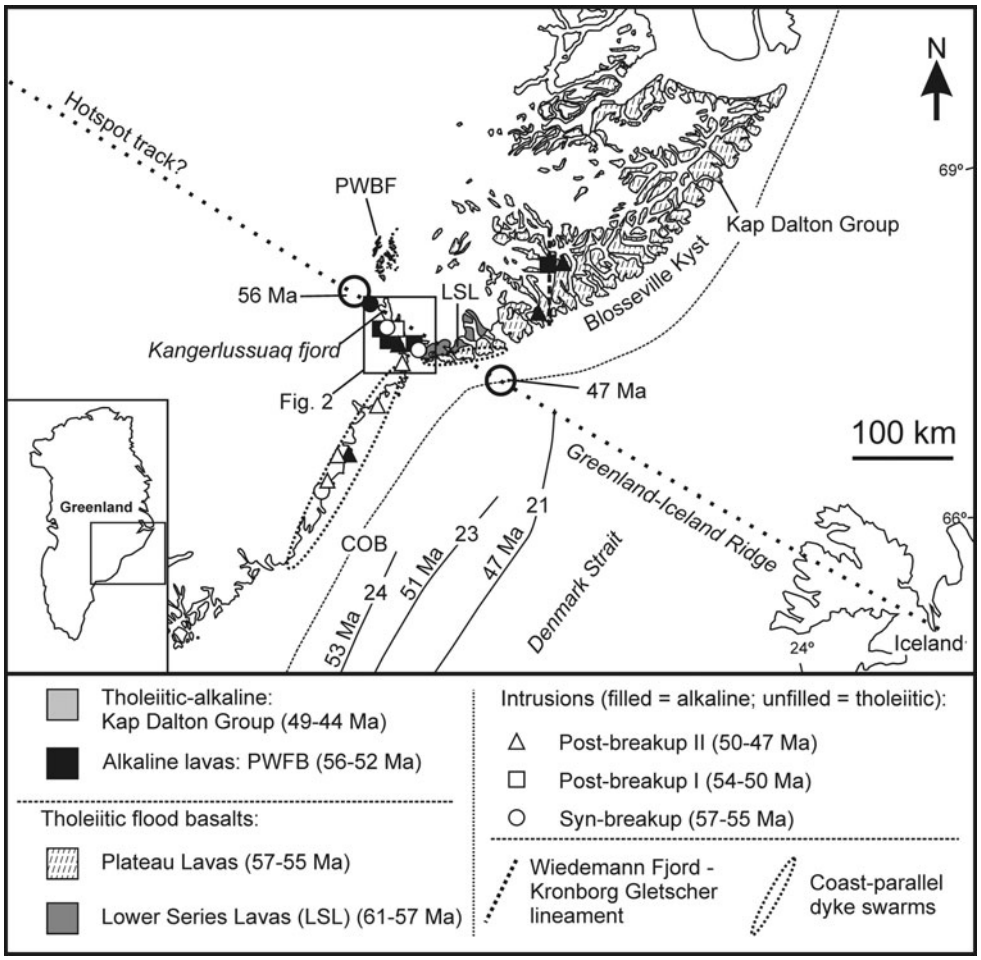

Figure 1. Simplified geological map of central East Greenland showing distribution of Palaeogene flood basalts and locations of major tholeiitic and alkaline intrusions arranged according to age. Only intrusions for which reliable radiometric data exist are shown. Post-47 Ma intrusions have been omitted for the sake of clarity. Base map modified after Myers, Dawes & Nielsen (1988) and Hansen *et al.* (2002). Age and compositional data from Nielsen (1987), Tegner *et al.* (1998, 2008), Peate *et al.* (2003), Storey, Duncan & Tegner (2007) and Larsen *et al.* (2013). Magnetic seafloor anomalies from Larsen (1990) illustrate location of spreading axis at 53, 51 and 47 Ma. Location of coast-parallel dyke swarms after Myers (1980) and Klausen & Larsen (2002). Dotted line shows possible hotspot track (modified from from Lawver & Müller, 1994) drawn to fit the Greenland–Iceland Ridge and the present-day position of the Iceland mantle plume beneath central Iceland. Proposed locations of the mantle plume axis at 56 and 47 Ma are shown by circles. COB – continent-ocean boundary; PWBF – Prinsen af Wales Bjerge Formation.

by the Kangerlussuaq Fjord, initially developed a rift-like structure accompanied by intrusion of tholeiitic dykes, but the rifting was aborted before it reached the oceanic stage (Brooks & Platt, 1975; Nielsen, 1987). The fjord has many of the characteristics of continental rift valleys and hosts more than twenty exposed intrusive complexes of both tholeiitic and alkaline affinities spanning 57 to 40 Ma. It includes one of the largest syenitic intrusions in the world, the c. 800 km^2 Kangerlussuaq Syenite (Wager, 1965; Brooks, 1973; Nielsen, 1987; Riishuus *et al.* 2008; Tegner *et al.* 2008). More importantly, the fjord includes intrusions emplaced between 54 and 50 Ma, that is, in the transition period between continental break-up and the proposed crossing of the rifted margin over the plume axis at 50–47 Ma. This period is otherwise characterized by a dearth of magmatic records (Holm, Heaman & Pedersen, 2006; Tegner *et al.* 2008; Holwell *et al.* 2012). The Kangerlussuaq Fjord therefore plays a key role in the magmatic evolution of East Greenland and presents an important link in understanding the rift-to-drift transition over the Iceland mantle plume during the opening of the North Atlantic Ocean.

Here we present isotope dilution thermal ionization mass spectrometry (ID-TIMS) U–Pb zircon ages from monzonites, syenites and alkali granites of the Kærven Complex, an early satellite intrusion of the Kangerlussuaq Syenite. The new ages are used in combination with published ages to refine and consolidate the magmatic history of the Kangerlussuaq Fjord and to re-evaluate the temporal and spatial pattern of post-break-up magmatism in relation to the Iceland hotspot track. Note that all uncertainties in the text are quoted at the 2σ level, and all cited $^{40}Ar/^{39}Ar$ ages are recalculated relative to the age of 28.201 Ma for the Fish Canyon sanidine standard and are normalized to a ^{40}K decay constant of 5.463×10^{-10} (Min *et al.* 2000; Kuiper *et al.* 2008).

https://doi.org/10.1017/S0016756815000448 Published online by Cambridge University Press

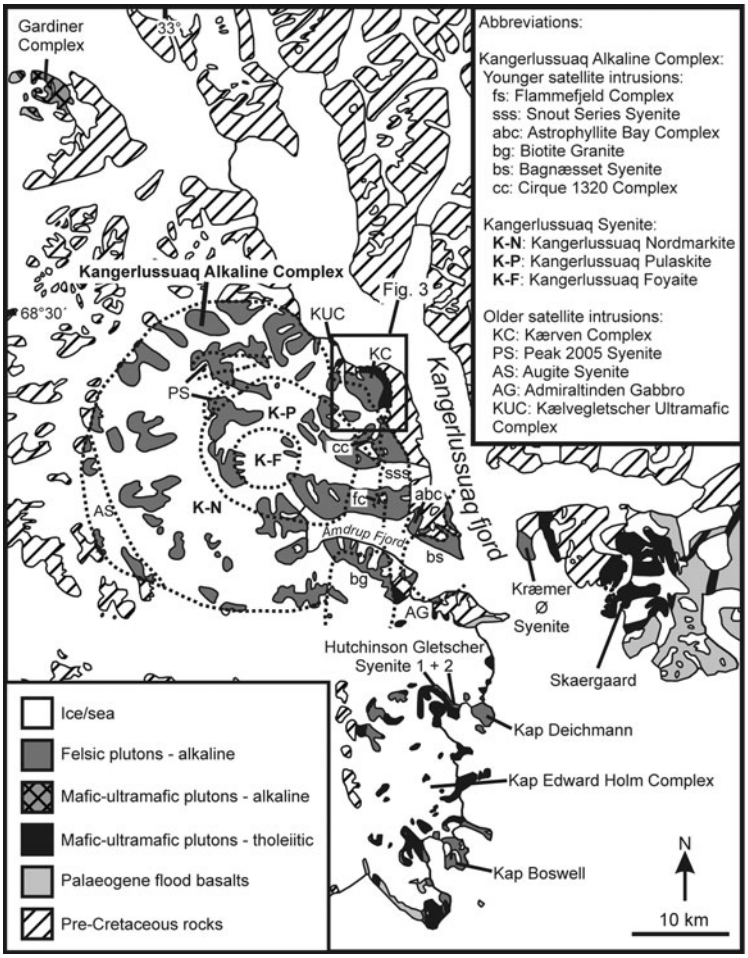

Figure 2. Geological map of the Kangerlussuaq Fjord, Greenland, showing major rock types and location of major plutons. Modified from Gleadow & Brooks (1979), Riishuus *et al.* (2006) and Tegner *et al.* (2008).

2. Geological background and previous geochronology

2.a. The Kangerlussuaq Fjord

The Kangerlussuaq Fjord is *c.* 80 km long and trends in a SSE-direction from the head of the fjord at *c.* 68° 38′ N and 32° 34′ W (Fig. 2). Palaeogene intrusions are abundant along the fjord in addition to several generations of dyke swarms (e.g. Brooks & Platt, 1975; Nielsen, 1978). Most of the intrusions were emplaced at, or close to, the unconformity between Archaean basement and overlying Palaeogene flood basalts (Wager, 1965; Nielsen, 1987). The alkaline Gardiner Complex is the northernmost intrusion (Fig. 2) and is dominated by ultramafic cumulates in addition to strongly undersaturated melilitolites, ijolites and carbonatites (Nielsen, 1987; Brooks, 2011). $^{40}Ar/^{39}Ar$ and Rb–Sr dating indicate emplacement between 56.9 ± 0.3 and 55.1 ± 1.2 Ma (Waight, Baker & Willigers, 2002; Tegner *et al.* 2008). An up to 150-m-thick sequence of alkaline lavas, formalized as the Prinsen af Wales Bjerge Formation and ranging in composition from nephelinite to trachybasalt, is exposed on nunataks 30–60 km further inland (Fig. 1; Hansen *et al.* 2002; Peate *et al.* 2003). The Prinsen af Wales Bjerge Formation is interbedded with the upper parts of the main sequence of break-up-related tholeiitic flood basalts exposed along the Blosseville coast, hereafter referred to collectively as the Plateau Lavas (Storey *et al.* 2007). $^{40}Ar/^{39}Ar$ dating indicates extrusion of the Prinsen af Wales Bjerge Formation between 55.2 ± 1.0 and 53.4 ± 1.2 Ma (Peate *et al.* 2003). The Kangerlussuaq Alkaline Complex (KAC) crops out 40–60 km SSE of the Gardiner Complex on the western side of the fjord and covers an area of more than 1000 km^2 (Fig. 2). The complex is predominately alkaline and radiometric dating indicates intrusion over an extended period between *c.* 55 and 40 Ma (Section 2.b). The Kræmer Ø syenite is located on the eastern side of the fjord (Fig. 2), *c.* 20 km from the coast, and has been dated to 50.7 ± 1.0 Ma by $^{40}Ar/^{39}Ar$ dating (Tegner *et al.* 2008). The tholeiitic Skaergaard intrusion crops out further SSE at the mouth of the fjord (Fig. 2). An age of 55.96 ± 0.02 Ma has recently been obtained for this intrusion by U–Pb zircon dating (Wotzlaw *et al.* 2012). This age is in good agreement with $^{40}Ar/^{39}Ar$ ages obtained by Hirschman *et al.* (1997) on hornblende (55.8 ± 0.3 Ma) and biotite (55.74 ± 0.14 Ma). The tholeiitic Kap Edward Holm layered gabbro is located across the fjord from the Skaergaard intrusion but is significantly younger, as indicated by $^{40}Ar/^{39}Ar$ ages of hornblende and biotite

https://doi.org/10.1017/S0016756815000448 Published online by Cambridge University Press

ranging from 50.8 ± 0.8 to 47.9 ± 0.6 Ma (Nevle *et al.* 1994; Tegner *et al.* 1998). The complex is intruded at its southern and northern perimeters by several syenitic intrusions (Kap Boswell, Kap Deichmann, Hutchinson Gletscher Syenite 1 and 2; Fig. 2). Hutchinson Gletscher Syenite 1 has been dated by the $^{40}Ar/^{39}Ar$ method to 45.4 ± 1.8 Ma (Nevle *et al.* 1994).

Coast-parallel tholeiitic dykes dominate at the mouth of the fjord (Fig. 1) and include three main swarms as mapped by Nielsen (1978): THOL-1, TRANS-1 and ALK-1. The tholeiitic THOL-1 dykes were emplaced before rifting and formation of a prominent coast-parallel flexure (Karson & Brooks, 1999) and have been interpreted as feeders to the Plateau Lavas. One of these dykes has been dated to 56.9 ± 1.2 Ma by Tegner *et al.* (1998). The TRANS-1 dykes are transitional between tholeiitic and alkaline compositions and comparable flood basalts have not been found in East Greenland (Hanghøj, Storey & Stecher, 2003). They are considered to be contemporaneous with the Kap Edward Holm Complex (Hanghøj, Storey & Stecher, 2003; Tegner *et al.* 2008), consistent with a $^{40}Ar/^{39}Ar$ age of 48.4 ± 2.8 Ma obtained on one of these dykes (Lenoir, Féraud & Geoffrey, 2003). The alkaline ALK-1 dykes have not been dated radiometrically, but cross-cutting relations indicate that they post-date the Kap Edward Holm Complex (Tegner *et al.* 2008). The coast-parallel dykes die out further inland where they are replaced by two radiating dyke swarms: THOL-2 and ALK-2 (Nielsen, 1978). The tholeiitic THOL-2 swarm is found in the outer and middle reaches of the Kangerlussuaq Fjord, but dies out north of the Kærven Complex (Fig. 2; Holm, Heaman & Pedersen, 2006). The dykes trend parallel to the fjord in the middle reaches of the fjord but have more variable trends in the outer parts, suggesting a radial pattern centred on the fjord mouth *c.* 10 km SW of the Skaergaard intrusion (Fig. 2; Nielsen, 1978). The dykes either cut or are cut by the Skaergaard intrusion, indicating syn-break-up emplacement at *c.* 56–55 Ma. This is consistent with an age of 54.7 ± 0.4 Ma obtained by U–Pb baddeleyite dating of a THOL-2 dyke by Holm, Heaman & Pedersen (2006; see Section 2.b). The ALK-2 dykes range in composition from alkali olivine basalt to trachyte (Brooks & Platt, 1975; Nielsen, 1978). The swarm has a radial pattern centred on the Amdrup Fjord area (Fig. 2; Nielsen, 1978). Zircon and titanite fission-track ages indicate emplacement between 41 and 36 Ma (Gleadow & Brooks, 1979).

2.b. The Kangerlussuaq Alkaline Complex (KAC)

The main constituent of the KAC is the roughly circular Kangerlussuaq Syenite (Fig. 2), which consists of an outer ring of nordmarkite (quartz alkali feldspar syenite), an inner ring of pulaskite (alkali feldspar syenite) and a core of foyaite (nepheline syenite) (Wager, 1965; Kempe, Deer & Wager, 1970; Brooks & Gill, 1982; Riishuus *et al.* 2008). The nordmarkite zone, which comprises *c.* 90 % of the intrusion (Wager, 1965), has been dated to 53 ± 6 Ma by whole-rock Rb–Sr dating (Holm, 1991). The pulaskite zone comprises *c.* 10 % of the complex and has been dated by several methods, including K–Ar, Rb–Sr mineral and whole-rock isochron dating; zircon and titanite fission-track dating; and $^{40}Ar/^{39}Ar$ biotite dating (Hamilton, 1966; Beckinsale, Brooks & Rex, 1970; Pankhurst, Beckinsale & Brooks, 1976; Gleadow & Brooks, 1979; Tegner *et al.* 2008). These methods have yielded ages clustering around 50 Ma but with errors that span 54–48 Ma. The $^{40}Ar/^{39}Ar$ age of 51.1 ± 1.1 Ma obtained by Tegner *et al.* (2008) is considered the most robust of these ages. The foyaite core comprises <1 % of the intrusion and has not been dated radiometrically.

The KAC also includes several smaller intrusions which have been referred to as satellite intrusions (Fig. 2), although the exact genetic relationship between the satellites and the Kangerlussuaq Syenite is unclear (Nielsen, 1987; Riishuus *et al.* 2006). The satellite intrusions either cut or are cut by the Kangerlussuaq Syenite and have accordingly been divided into younger and older satellites, respectively.

The older satellites include the Kælvegletscher Ultramafic Complex, Admiraltinden Gabbro, Augite Syenite, Peak 2005 Syenite and the Kærven Complex (Fig. 2). The Kærven Complex crops out over a *c.* 10 km^2 area at the northeast corner of KAC and is cut by the Kangerlussuaq Syenite along a *c.* 5-km-long, NW–SE-trending semi-linear contact (Fig. 3). The crescent-shaped Kærven Gabbro forms the eastern and oldest part of the Kærven Complex. The gabbro consists of several intrusive units with tholeiitic hypersthene-gabbro as the dominant rock type (Deer & Kempe, 1976; Holm, Heaman & Pedersen, 2006). To the north the gabbro cuts a small ultramafic intrusion of tholeiitic affinity (Holm & Prægel, 2006) and to the east it cuts an east–west-striking tholeiitic dyke, which in turn cuts a fjord-parallel tholeiitic dyke further east (Fig. 3). The latter is inferred to be part of the THOL-2 dyke swarm and a U–Pb baddeleyite age of 54.7 ± 0.4 Ma has been obtained for the dyke by Holm, Heaman & Pedersen (2006). The gabbro itself yields $^{40}Ar/^{39}Ar$ biotite and U–Pb zircon ages of 55.5 ± 1.4 and 53.0 ± 0.3 Ma, respectively (Fig. 3; Holm, Heaman & Pedersen, 2006; Tegner *et al.* 2008). To the west the gabbro is cut by a series of alkaline intrusions grading westwards from monzonite through syenite to alkali granite (Fig. 3). Two of the felsic intrusions gave $^{40}Ar/^{39}Ar$ amphibole ages of 54 ± 2 and 53.1 ± 1.3 Ma (Fig. 3; Holm, 1991; Tegner *et al.* 2008).

The younger satellites include the Cirque 1320 Complex, Astrophyllite Bay Complex, Snout Series Granite, Biotite Granite, Bagnæsset Syenite Complex and Flammefjeld Complex (Fig. 2). These intrusions are concentrated around the Amdrup Fjord at the southeast margin of the KAC, and geochronology data indicate that most were emplaced between 46 and 48 Ma (Riishuus *et al.* 2005; Tegner *et al.* 2008). Exceptions are the Cirque 1320 and Flammefjeld complexes, for which Re–Os molybdenite ages of 52.7 ± 0.3 and 39.7 ± 0.2 Ma

https://doi.org/10.1017/S0016756815000448 Published online by Cambridge University Press

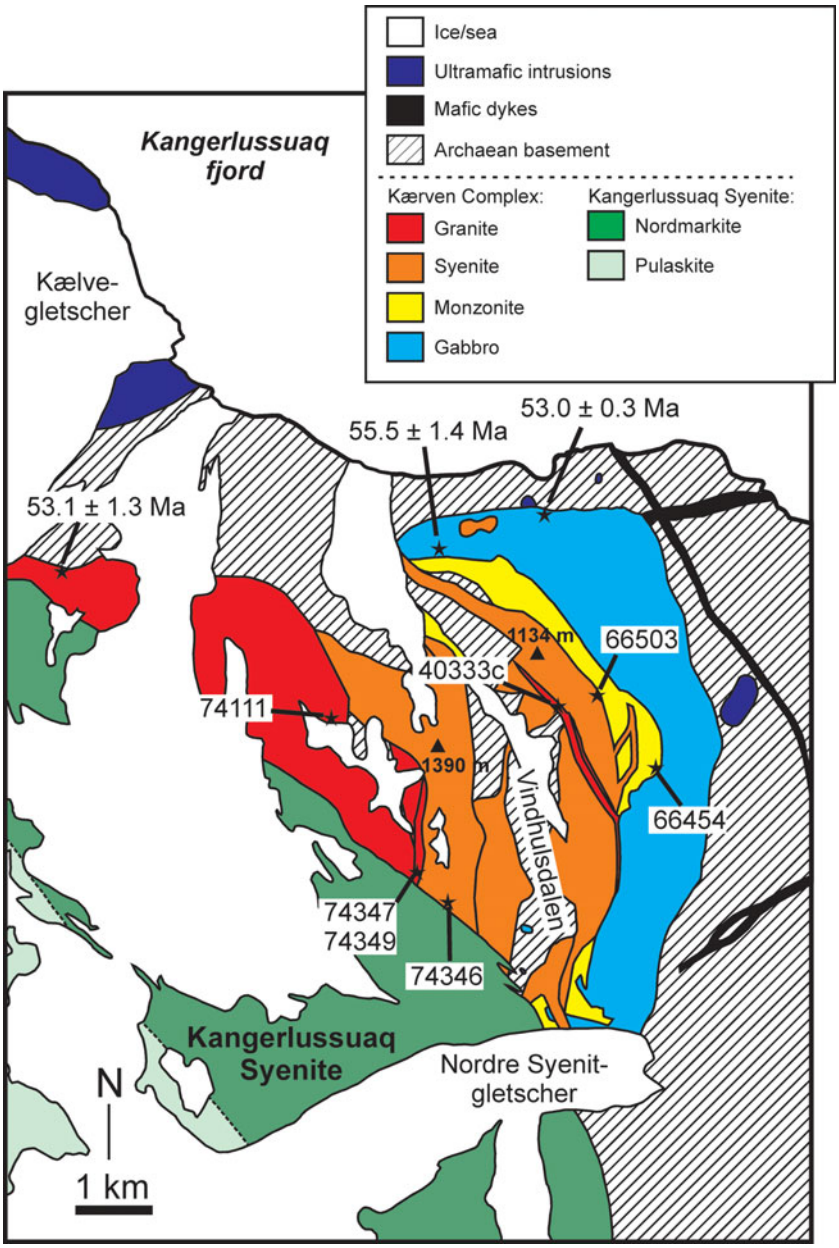

Figure 3. (Colour online) Geological map of the Kærven Complex showing major intrusive units and location of the dated samples. Location and ages of previously dated samples are also shown. Age data from Holm, Heaman & Pedersen (2006) and Tegner *et al.* (2008).

have been obtained (Brooks *et al.* 2004; Holwell *et al.* 2012).

3. Samples and intrusive units

Seven samples from six different intrusive units of the Kærven Complex were dated in this study by the ID-TIMS U–Pb technique (Fig. 3). The samples were selected with the aim of covering most of the major intrusive units of the complex. The dated units are monzonitic to granitic (SiO_2 = 62–72 wt %; Fig. 4) and are exposed on either side of the Vindhulsdalen Valley (Fig. 3). They have accordingly been grouped into East and West units. The dated samples are metaluminous to weakly peralkaline [(Na + K)/Al = 0.76–1.01] and are characterized by high alkali contents (Fig. 4) and high Fe/(Fe + Mg) ratios (0.82–0.95) typical of ferroan, A-type granitoids (Frost & Frost, 2008).

East Monzonite (sample 66454) is the easternmost felsic unit of the Kærven Complex and comprises several thin, monzonitic dykes emplaced along the western margin of the Kærven Gabbro (Fig. 3). The dykes can be seen cutting the Kærven Gabbro and locally contain gabbroic inclusions, indicating that the monzonite dykes are younger than the gabbro. The dated sample is porphyritic with *c.* 15 % phenocrysts of patch perthite alkali feldspar (up to 8 mm long) enclosed in a medium-grained groundmass of plagioclase, microperthite, quartz, amphibole, clinopyroxene, biotite, Fe-Ti oxide, zircon and titanite (in order of decreasing abundance; see also online Supplementary Fig. S1a, available at http://journals.cambridge.org/geo).

https://doi.org/10.1017/S0016756815000448 Published online by Cambridge University Press

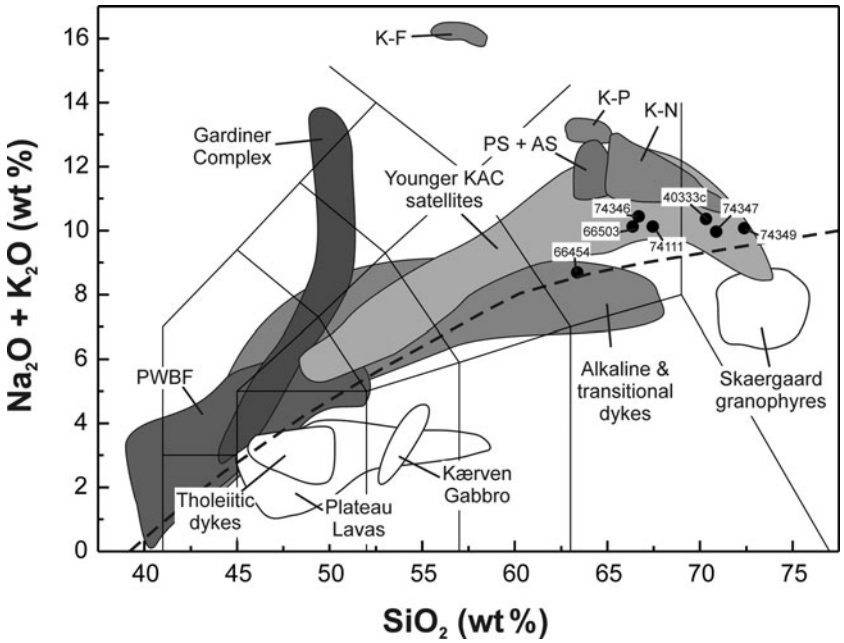

Figure 4. Whole-rock compositions of the Kangerlussuaq Fjord plotted in the total alkalis vs. silica classification diagram (Le Maitre *et al.* 2002). Alkaline–tholeiitic division line (dashed line) is from Irvine & Baragar (1971). Tholeiitic rocks are shown as white fields. Alkaline rocks are shown as grey fields. Samples dated in this study are shown as black dots. Abbreviations: PS + AS – Peak 2005 Syenite and Augite Syenite (older satellites of the KAC); PWBF – Prinsen af Wales Bjerge Formation; K-F – Kangerlussuaq Foyaite; K-P – Kangerlussuaq Pulaskite; K-N – Kangerlussuaq Nordmarkite. Younger KAC satellites include the Cirque 1320 Complex, Snout Series Syenite, Astrophyllite Bay Complex, Biotite Granite and Bagnæsset Syenite. Skaergaard granophyre data is from podiform pegmatites and segregation veins of the Skaergaard intrusion. The granophyres record late-stage fractionates of the Skaergaard melt (Larsen & Brooks, 1994) and exemplify the evolved rocks of the tholeiitic trend. Alkaline and transitional dykes include the ALK-1, ALK-2 and TRANS-1 dyke swarms of Nielsen 1978. Tholeiitic dykes include the THOL-1 and THOL-2 swarms. Data compiled from Nielsen (1978, 1987), McBirney (1989), Larsen & Brooks (1994), Hansen *et al.* (2002), Peate & Stecher (2003), Peate *et al.* (2003), Andreasen, Peate & Brooks (2004), Riishuus *et al.* (2005, 2006, 2008) and Holm, Heaman & Pedersen (2006).

East Syenite (sample 66503) is a red-brown, 250–300-m-wide syenitic dyke, which cuts both the East Monzonite and the Kærven Gabbro (Fig. 3). The syenite is coarse-grained and composed of microperthite, quartz, amphibole, fayalite, Fe-Ti oxide, clinopyroxene, zircon and apatite (online Supplementary Fig. S1b, available at http://journals.cambridge.org/geo).

East Granite (sample 40333c) is a 20–30-m-wide alkali granite dyke. The dyke intrudes the north–south-trending contact between the Kærven Gabbro and the East Syenite in the southern part of the complex (Fig. 3). It follows this contact for *c.* 1 km before turning northwest and cutting across the East Syenite in the central part of the complex. The rock is yellowish-white to light grey or pink in colour, with *c.* 10 % phenocrysts of microperthite (typically 3–4 mm long) in a medium-grained groundmass of microperthite, quartz, amphibole, clinopyroxene, Fe-Ti oxide and zircon (online Supplementary Fig. S1c, available at http://journals.cambridge.org/geo).

West Granite 1 (sample 74111) crops out in the area south and west of the 1390 m western peak of Kærven (Fig. 3). The coarse-grained rock has a distinctive red colour and is composed of microperthite, quartz, amphibole, clinopyroxene, Fe-Ti oxide, fayalite, biotite and zircon (online Supplementary Fig. S2a, available at http://journals.cambridge.org/geo).

West Granite 2 (samples 74347 and 74349) is a *c.* 200-m-wide, north–south-trending, alkali granite dyke intruded into the southeast margin of West Granite 1 (Fig. 3). The dyke has *c.* 5 % phenocrysts of microperthite (3–4 mm) in a medium-grained groundmass of microperthite, quartz, amphibole, Fe-Ti oxide, biotite and zircon (online Supplementary Fig. S2b, available at http://journals.cambridge.org/geo).

West Syenite (sample 74346) forms a *c.* 600-m-wide syenitic dyke. In the southern part of the complex the dyke trends *c.* north–south and is emplaced between West Granite 2 to the west and an older syenitic dyke of comparable width to the east (Fig. 3). The latter can be followed northeast across the Vindhulsdalen Valley, where it is cut by the East Granite unit. Further north the West Syenite changes to a NW–SE trend and is observed cutting West Granite 1. The rock is coarse grained and composed of microperthite, amphibole, Fe-Ti oxide, clinopyroxene, apatite and zircon (online Supplementary Fig. S2c, available at http://journals.cambridge.org/geo).

4. Analytical details

The samples were crushed and processed through a combination of panning, magnetic (Frantz isodynamic separator) and density (methylene iodide) separation

https://doi.org/10.1017/S0016756815000448 Published online by Cambridge University Press

Table 1. Pb isotopic compositions of alkali feldspar separates from the Kærven Complex

Sample no.	Rock type	$^{206}Pb/^{204}Pb$	$^{207}Pb/^{204}Pb$	$^{208}Pb/^{204}Pb$
40228fsp	Monzonite	15.16	14.857	37.21
40271fsp	Monzonite	15.75	14.947	36.97
66550fsp	Monzonite	15.64	14.935	37.39
66497fsp	Syenite	16.23	15.038	36.98
66525fsp	Syenite	16.19	15.006	36.84
66520fsp	Syenite	16.21	15.021	36.84
66495fsp	Alkali granite	16.16	14.985	36.82
66551fsp	Alkali granite	16.30	15.050	37.02

Feldspar separates were analysed using a VG Sector 54 TIMS at the University of Copenhagen following standard dissolution and ion exchange procedures. The data were corrected for mass fractionation using a value of 0.12 ± 0.02 (2σ) % amu^{-1} based on replicate measurements of the NBS981 standard and the values of Todt *et al.* (1996).

techniques at the University of Copenhagen to yield heavy mineral concentrates. Zircons of similar size, shape and colour were then handpicked under a binocular microscope to produce a set of homogeneous, multi-grain aliquots.

The U–Pb analytical work was carried out at the University of Alberta and followed the procedures described in detail by Heaman, Erdmer & Owen (2002). The selected zircon fractions were washed in warm 4N HNO_3 prior to weighing with a UTM ultramicrobalance. The samples were spiked with a mixed ^{205}Pb–^{235}U tracer solution and dissolved in a HF–HNO_3 mixture in teflon bombs at 230 °C. Purified Pb and U aliquots were analysed on a VG354 multi-collector thermal ionization mass spectrometer (TIMS) using operating conditions outlined in Heaman *et al.* (2002). All isotopic data were corrected for mass fractionation using the following values determined from the long-term reproducibility of the NBS981 and NBS U500 standards: 0.10 % per atomic mass unit (amu^{-1}) for Pb and 0.12 % amu^{-1} for U. Blank correction was 2 ± 1 pg Pb and 0.5 ± 0.25 pg U, consistent with routine blank levels at the University of Alberta (Heaman *et al.* 2011).

Common Pb in excess of blank was corrected for using compositions estimated from Pb isotopic analyses of alkali feldspar separates from the Kærven Complex (Table 1). The feldspars are characterized by low Pb isotope ratios and are considerably less radiogenic than Icelandic lavas (e.g. Hanan & Schilling, 1997; Stracke *et al.* 2003). Similar compositions have been reported from flood basalts and dykes in the Kangerlussuaq area, and from the Kælvegletscher Ultramafic Complex of the KAC (Figs 2, 3). The un-radiogenic Pb isotope compositions have been interpreted to reflect contamination of Iceland plume magmas by Archaean continental crust and/or contributions from metasomatized continental lithospheric mantle (e.g. Hansen & Nielsen, 1999; Hanghøj, Storey & Stecher, 2003; Holm & Prægel, 2006; Peate *et al.* 2008). Sample 66454 (East Monzonite) has been corrected using the composition: $^{206}Pb/^{204}Pb = 15.5 \pm 0.6$ and $^{207}Pb/^{204}Pb = 14.91 \pm 0.10$ (average of three monzonite samples from East Kærven; Table 1). All other samples have been corrected using the composition: $^{206}Pb/^{204}Pb = 16.22 \pm 0.11$; $^{207}Pb/^{204}Pb = 15.02 \pm 0.05$ (average of five syenite and granite samples from East and West Kærven).

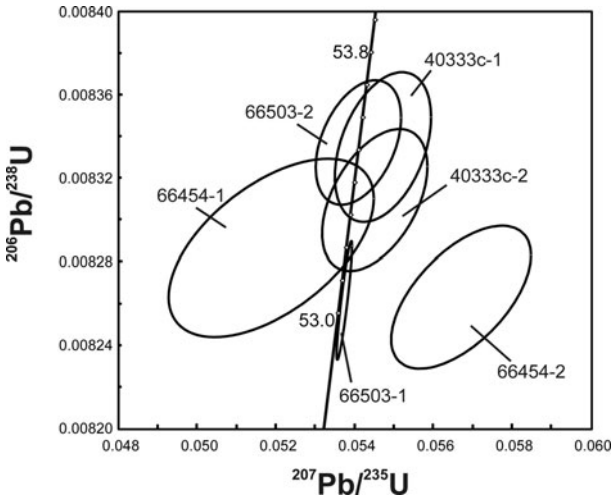

Figure 5. Wetherill concordia diagram showing U–Pb results of zircon fractions from East Kærven.

A correction for ^{230}Th disequilibrium has been applied using the equation of Schärer (1984) and assuming a Th/U_{magma} ratio of 5 (average value estimated from whole-rock data). Calculations indicate that the correction is robust to large variations in magmatic Th/U. The correction increases the $^{206}Pb/^{238}U$ age by *c.* 0.1 Ma for all fractions, except the high Th/U fraction 74347–2 (Table 2) for which the correction is negligible. The overall effect of the correction is to increase the degree of concordance.

Data plotting and age calculations were performed with the ISOPLOT software of Ludwig (2003) using decay constants of 1.55125×10^{-10} a^{-1} (^{238}U) and 9.8485×10^{-10} a^{-1} (^{235}U) and a $^{238}U/^{235}U$ ratio of 137.88 as recommended by Steiger & Jäger (1977). The uncertainties listed in Table 2 were calculated by propagation of all known sources of error and are quoted at the 2σ level.

5. U–Pb results

5.a. East Monzonite (sample 66454)

Two multi-grain zircon fractions were analysed from this sample. Fraction 66454–1 consists principally of euhedral, prismatic crystals, 100–200 μm long with a predominance of {100} and {101} crystal faces. The zircons of 66454–2 are more equant and show a combination of {100}, {110} and {101} crystal faces. The two fractions are characterized by very low U (58 and 45 ppm) and Pb (<1 ppm) contents and relatively high Th/U ratios (0.94 and 0.85; Table 2). Fraction 66454–1 plots within error of the concordia curve with a $^{206}Pb/^{238}U$ age of 53.2 ± 0.2 Ma (Fig. 5). Fraction 66454–2 yields a $^{206}Pb/^{238}U$ age of 53.0 ± 0.2 Ma,

https://doi.org/10.1017/S0016756815000448 Published online by Cambridge University Press

Table 2. ID-TIMS U–Pb zircon results from the Kærven Complex

Fraction	Intrusive unit	Description[a]	Weight (μg)	Size[b] (μm)	U (ppm)	Th/U[c]	Pb (ppm)	TCPb[d] (pg)	$^{206}Pb/^{204}Pb$	$^{206}Pb/^{238}U$	±2σ (abs)	$^{207}Pb/^{235}U$	±2σ (abs)	ρ	$^{207}Pb/^{206}Pb$	±2σ (abs)	$^{206}Pb/^{238}U$ age (Ma)	±2σ	$^{207}Pb/^{235}U$ age (Ma)	±2σ
East Kærven																				
66454–1	East Monzonite	cl, eu, pr [40]	104.1	100–200	58	0.94	0.6	11	305	0.008286	0.000035	0.0519	0.0021	0.55	0.0454	0.0018	53.2	0.2	51.4	2.1
66454–2	East Monzonite	cl, eu, eq [32]	108.5	100–200	45	0.85	0.5	14	201	0.008263	0.000028	0.0567	0.0015	0.43	0.0498	0.0012	53.0	0.2	56.0	1.4
66503–1	East Syenite	cl, eu, pr-eq [22]	266.2	150–300	448	0.71	4.1	12	5108	0.008261	0.000023	0.05374	0.00017	0.91	0.047182	0.000059	53.0	0.1	53.2	0.2
66503–2	East Syenite	cl, eu, pr-eq + fr [37]	140.3	100–200	341	0.68	3.2	10	2632	0.008337	0.000024	0.05410	0.00088	0.40	0.04707	0.00072	53.5	0.2	53.5	0.9
40333c-1	East Granite	cl, eu, pr [45]	59.1	75–175	368	0.61	3.4	8	1479	0.008335	0.000030	0.05472	0.00099	0.40	0.04762	0.00081	53.5	0.2	54.1	1.0
40333c-2	East Granite	cl, eu, pr [40]	20.3	50–125	282	0.69	2.7	6	532	0.008309	0.000028	0.0545	0.0011	0.47	0.04758	0.00089	53.3	0.2	53.9	1.1
West Kærven																				
74411–1	West Granite 1	cl, sub, pr + fr [40]	59.5	75–200	337	0.87	9.2	362	47	0.008805	0.000065	0.0770	0.0033	0.31	0.0634	0.0026	56.5	0.4	75.3	3.1
74411–2	West Granite 1	cl, sub, pr + fr [60]	107.4	75–175	487	0.77	4.8	30	933	0.008362	0.000018	0.05465	0.00030	0.49	0.04740	0.00023	53.7	0.1	54.0	0.3
74347–1	West Granite 2	cl, eu, pr + fr [45]	23.7	50–125	390	0.51	3.9	14	356	0.008282	0.000029	0.0563	0.0014	0.47	0.0493	0.0011	53.2	0.2	55.6	1.3
74347–2	West Granite 2	cl, eu, pr + fr [45]	27.5	50–125	970	7.70	208	200	577	0.06716	0.00076	0.799	0.076	0.82	0.0863	0.0074	419	4.6	597	42.4
74349–1	West Granite 2	cl, eu, pr [45]	24.0	75–150	293	0.63	4.2	41	107	0.00838	0.00013	0.0605	0.0097	0.64	0.0524	0.0079	53.8	0.8	60	9.3
74349–2	West Granite 2	cl, eu, pr + fr [40]	33.8	75–175	307	0.53	3.0	8	679	0.008604	0.000026	0.0576	0.0010	0.43	0.04852	0.00079	55.2	0.2	56.8	1.0
74346–1	West Syenite	y, sub, pr-eq + fr [21]	87.5	125–200	240	0.37	2.5	51	225	0.008149	0.000028	0.0540	0.0011	0.38	0.04807	0.00095	52.3	0.2	53.4	1.1
74346–2	West Syenite	y, sub, pr-eq [50]	66.5	75–150	118	0.43	1.5	39	121	0.008288	0.000039	0.0573	0.0032	0.65	0.05016	0.00263	53.2	0.3	56.6	3.0

Atomic ratios are corrected for spike, blank and common Pb (see Table 1). Blank composition: $^{206}Pb/^{204}Pb = 18.24 \pm 0.07$; $^{207}Pb/^{204}Pb = 15.64 \pm 0.06$; $^{208}Pb/^{204}Pb = 37.50 \pm 0.15$. $^{206}Pb/^{238}U$ and $^{206}Pb/^{207}Pb$ values have been corrected for excess ^{206}Pb assuming Th/U = 5 for the parent magma and using the equation of Schärer (1984). [a]cl – colourless; y – yellow; eu – euhedral; sub – subhedral, pr – prismatic; eq – equant; fr – fragments; [40] number of grains in fraction; [b]longest dimension; [c]thorium concentration is estimated from amount of ^{208}Pb and $^{206}Pb/^{238}U$ age; and [d]TCPb = total common Pb (initial + blank).

within error of fraction 66454–1. The latter is normally discordant and plots at a high angle to the concordia, which may indicate minor inheritance coupled with Pb loss.

5.b. East Syenite (sample 66503)

The zircons recovered from sample 66503 range from *c.* 100 to 300 μm in length and are generally colourless, euhedral, equant to prismatic crystals showing a combination of {101}, {100} and {110} crystal faces. The larger grains were sampled in fraction 66503–1, whereas the smaller grains were sampled in fraction 66503–2. The fractions have low to moderate U and Th contents (U = 341–448 ppm; Th/U = 0.68–0.71; Table 2). Fraction 66503–1 plots slightly to the right of the concordia with a $^{206}Pb/^{238}U$ age of 53.0 ± 0.2 Ma (Fig. 5). Fraction 66503–2 is concordant and yields a $^{206}Pb/^{238}U$ age of 53.5 ± 0.2 Ma. The spread in $^{206}Pb/^{238}U$ ages could be due to minor Pb loss or recycling of antecrysts (e.g. Miller & Wooden, 2004; Miller *et al.* 2007).

5.c. East Granite (sample 40333c)

The zircon crystals extracted from sample 40333c form a fairly homogeneous population of small (55–175 μm long), euhedral, prismatic grains with a predominance of {100} and {101} crystal faces (see online Supplementary Fig. S3a, available at http://journals.cambridge.org/geo). The crystals are generally colourless and clear, although some contain small needle-shaped mineral inclusions. The zircons have relatively low U and Th contents (U = 282–368 ppm; Th/U = 0.61–0.69; Table 2). The two analysed fractions plot within error of each other and yield a combined concordia age of 53.4 ± 0.1 Ma (MSWD = 1.6, concordance + equivalence; Fig. 5). This age is within error of an $^{40}Ar/^{39}Ar$ age (54 ± 2 Ma) obtained on amphibole from the same sample (Holm, 1991).

5.d. West Granite 1 (sample 74411)

The zircons recovered from sample 74111 are morphologically similar to the zircons of 40333c; they are slightly turbid and more subhedral however, and prism fragments are more common (see online Supplementary Fig. S3b, available at http://journals.cambridge.org/geo). The analysed fractions have low to moderate U and Th contents (U = 387–487 ppm; Th/U = 0.77–0.88; Table 2). The discordant fraction 74111–1 yields a $^{206}Pb/^{238}U$ age of 56.5 ± 0.4 Ma (not shown). The analysis is compromised by a high common Pb content (362 pg Pb), making it highly sensitive to the common Pb correction. We suspect that this may be due to laboratory contamination and the fraction will therefore not be considered further. Fraction 74111–2 plots within error of the concordia with a $^{206}Pb/^{238}U$ age of 53.7 ± 0.1 Ma (Fig. 6). This fraction also has a relatively high common Pb content (30 pg Pb), but has a much higher proportion of radiogenic Pb ($^{206}Pb/^{204}Pb$ = 933) and is therefore less sensitive to the common Pb correction. For example, the $^{206}Pb/^{238}U$ age decreases by a maximum of 0.1 Ma if up to 30 pg Pb blank is assumed.

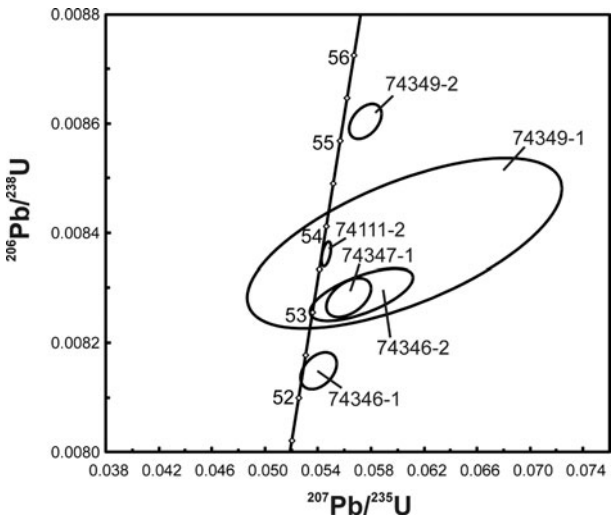

Figure 6. Wetherill concordia diagram showing U–Pb results of zircon fractions from West Kærven.

5.e. West Granite 2 (samples 74347 and 74349)

Zircons from sample 74349 occur as colourless, euhedral, slender prisms (75–175 μm) with a predominance of {100} and {101} crystal faces (see online Supplementary Fig. S3c; available at http://journals.cambridge.org/geo). The analysed fractions have low U and Th contents (U = 293–307 ppm; Th/U = 0.53–0.63). Fraction 74349–1 is within error of the concordia with a $^{206}Pb/^{238}U$ age of 53.8 ± 0.8 Ma (Fig. 6). The large age uncertainty reflects a proportionally low content of radiogenic Pb (64 % of total Pb) and a small sample size. The discordant fraction 74349–2 yields a somewhat older $^{206}Pb/^{238}U$ age of 55.2 ± 0.2 Ma, presumably due to inheritance.

Zircons from sample 74347 are slightly shorter (50–125 μm) than the zircons from 74349 but are otherwise morphologically similar. Fraction 74347–2 has the highest U and Th contents observed in this study (U = 970 ppm; Th/U = 7.7) and is highly discordant with a $^{207}Pb/^{206}Pb$ age of 1346 ± 161 Ma, indicating inclusion of an inherited Precambrian component. Fraction 74347–1 is also discordant, but markedly less so than fraction 74347–2 and yields a $^{206}Pb/^{238}U$ age of 53.2 ± 0.2 Ma (Fig. 6).

5.f. West Syenite (sample 74346)

Fractions 74346–1 and 74346–2 are characterized by yellowish, prismatic to equant, subhedral zircons dominated by {100} and {101} crystal faces. The analysed fractions have low U and Th contents (U = 118–240 ppm; Th/U = 0.37 and 0.43). The U–Pb results

https://doi.org/10.1017/S0016756815000448 Published online by Cambridge University Press

are within error of the concordia curve, albeit marginally so (<5 % probability of concordance), and yield $^{206}Pb/^{238}U$ ages of 52.3 ± 0.2 and 53.2 ± 0.3 Ma, respectively (Fig. 6). The age spread may reflect Pb loss and/or recycling of antecrysts.

6. Discussion

6.a. Age constraints from the Kærven Complex

Concordant analyses from East Kærven yield $^{206}Pb/^{238}U$ ages between 53.5 ± 0.2 and 53.2 ± 0.2 Ma. Absolute age differences could not be resolved with the technique used in this study, suggesting intrusion within a relatively short time span (*c.* 100–200 ka). Cross-cutting relationships, however, indicate that the East Granite is the youngest of the dated East Kærven units, whereas the East Monzonite is the oldest. The concordia age of the East Granite (53.4 ± 0.1 Ma) unit is within error of a previous $^{40}Ar/^{39}Ar$ age estimate (Holm, 1991); we therefore consider this a robust minimum age for the East Kærven units and propose that most of East Kærven was emplaced between *c.* 53.5 and 53.3 Ma. The $^{206}Pb/^{238}U$ ages from East Kærven are younger than the 55.5 ± 1.4 Ma $^{40}Ar/^{39}Ar$ age obtained by Tegner *et al.* (2008) for the Kærven Gabbro and is consistent with field relations, which indicate that the East Kærven units post-date the gabbro. However, U–Pb baddeleyite dating of a gabbro pegmatite from the northern margin of the Kærven Gabbro (Fig. 3) has yielded an age of 53.0 ± 0.3 Ma (Holm, Heaman & Pedersen, 2006), indicating that gabbroic magmatic activity continued penecontemporaneously with intrusion of the East Kærven units. Intrusion of the gabbro pegmatite, however, does not appear to have affected the K–Ar system of the gabbro sample dated by Tegner *et al.* (2008). We therefore surmise that the gabbro pegmatite records a relatively small pulse of mafic magma intruded after most of the gabbro had cooled below the closure temperature for Ar in biotite (*c.* 300 °C; McDougall & Harrison, 1988).

Concordant analyses from West Kærven yield ages between 53.8 ± 0.8 and 52.3 ± 0.3 Ma and are within error of an $^{40}Ar/^{39}Ar$ age of 53.1 ± 1.3 Ma obtained from the westernmost Kærven unit by Tegner *et al.* (2008) (Fig. 3). The U–Pb ages mostly overlap with the ages from East Kærven and suggest coeval emplacement of the East and West Kærven units. The West Syenite could be slightly younger, but the data are inconclusive due to a large spread in $^{206}Pb/^{238}U$ ages.

6.b. Age of the Kangerlussuaq Syenite

The Kærven Complex is cut to the south by the Kangerlussuaq Syenite (Figs 2, 3). The syenite was originally mapped by Wager (1965) who noted a lack of internal intrusive contacts and interpreted the intrusion to have formed by fractional crystallization inwards from the margins of a single large magma chamber. Kempe *et al.* (1970) later reported gradational variations in modal contents between the different zones mapped by Wager (1965), and concurred with a temporal evolution from early (outer) nordmarkite to late (inner) pulaskite and foyite.

A more complicated model is presented by Riishuus *et al.* (2008) involving concurrent assimilation and fractional crystallization and recharge with more primitive magma, but with the same overall temporal pattern. However, Holm, Prægel & Egeberg (1991) report abrupt rather than gradual changes in mineralogy as the nordmarkite-pulaskite boundary is traversed and propose that the Kangerlusuaq Syenite is in fact composed of a number of discrete intrusive units. This is supported by the occurrence of intrusive sheets of pulaskite within the nordmarkite zone in the Amdrup Fjord region (C.K. Brooks, personal communication cited in Nielsen 1987). Unfortunately, most efforts on dating the Kangerlussuaq Syenite have focused on the pulaskite zone; the 53 ± 6 Ma whole-rock Rb–Sr age of Holm (1991) is to our knowledge the only radiometric age from the nordmarkite zone. A maximum age of *c.* 53.5 Ma is however provided by the U–Pb results for East Kærven and minimum age constraints are provided by the satellite complexes that intrude the eastern margin of the Kangerlussuaq Nordmarkite. Existing geochronlogical data indicates that most of the younger satellites were intruded between 48 and 46 Ma.

However, Holwell *et al.* (2012) recently obtained a Re–Os age of 52.7 ± 0.3 Ma for molybdenite-bearing quartz veins cutting the Cirque 1320 Complex (Fig. 2). This method has been shown to be a remarkably robust chronometer under almost all geological conditions when applied to molybdenite (Stein *et al.* 2001). The Re–Os age is significantly older than the 51.1 ± 1.1 Ma $^{40}Ar/^{39}Ar$ age reported by Tegner *et al.* (2008) on biotite from the Kangerlussuaq Pulaskite. However, given the relatively low closure temperature for Ar in biotite and the size of the Kangerlussuaq Syenite, the $^{40}Ar/^{39}Ar$ age should probably be considered a cooling age rather than a crystallization age.

We therefore infer that the Kangerlussuaq Nordmarkite was intruded between *c.* 53.5 and 52.7 Ma. If the single-intrusion model (e.g. Wager 1965; Riishuus *et al.* 2008) is correct, then the age of the nordmarkite can be considered representative of the entire Kangerlussuaq Syenite. If not (e.g. Holm, 1991), we opine that the pulaskite, and possibly also the foyaite, was intruded penecontemporaneously with the nordmarkite, although more precise age determinations of the pulaskite are required for confirmation. The ages of the Augite and Peak 2005 Syenite intrusions (Fig. 1), which pre-date the Kangerlussuaq Syenite, are not well constrained. However, based on geochemical similarities (Riishuus *et al.* 2006), we infer that they were intruded shortly before the Kangerlussuaq Syenite. We therefore propose that most of the alkaline part of the KAC was intruded between *c.* 53.5 and 52.7 Ma, prior to the crossing of the rifted margin over the axis of the

https://doi.org/10.1017/S0016756815000448 Published online by Cambridge University Press

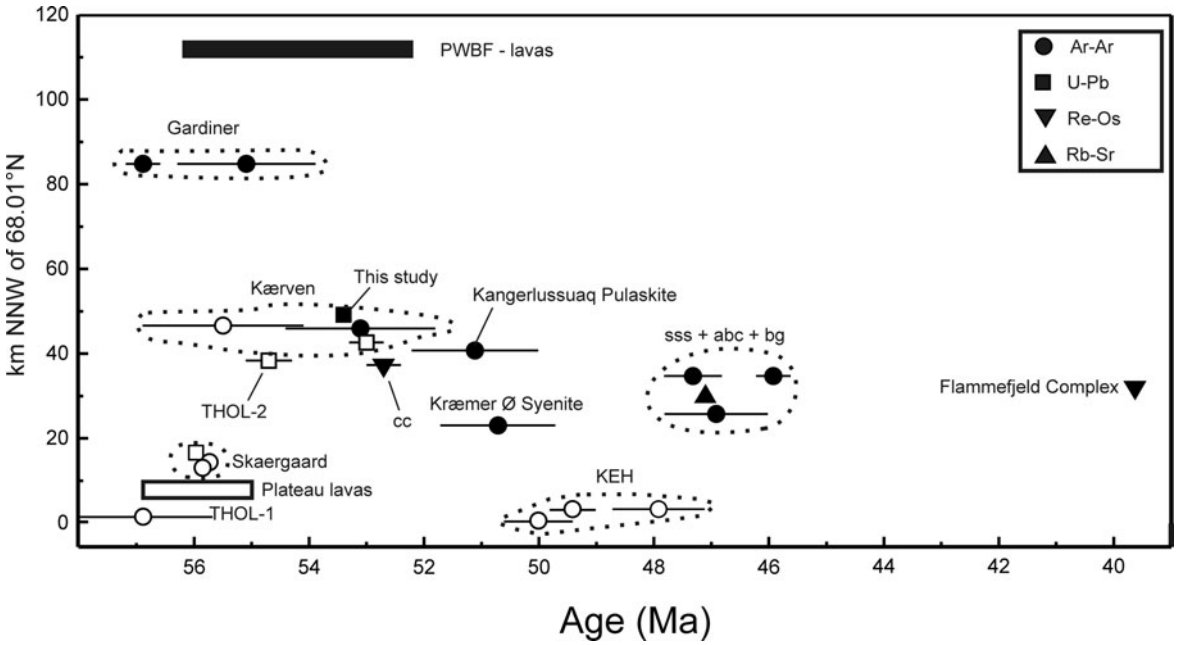

Figure 7. Summary of precise (≤2.5 % 2σ error) U–Pb, $^{40}Ar/^{39}Ar$, Rb–Sr and Re–Os ages for alkaline (filled symbols) and tholeiitic (unfilled symbols) intrusions of the Kangerlussuaq Fjord compiled from the literature. Data from Nevle *et al.* (1994), Hirschman *et al.* (1997), Tegner *et al.* (1998, 2008), Riishuus *et al.* (2005), Holm, Heaman & Pedersen (2006), Holwell *et al.* (2012), Wotzlaw *et al.* (2012) and this study (concordia age for East Granite). Error bars indicate 2σ errors. Also shown are age ranges of Plateau Lavas (tholeiitic) and Prinsen af Wales Bjerge Formation (PWBF) lavas (alkaline) (including 2σ errors; data from Peate *et al.* 2003; Storey, Duncan & Tegner 2007). Age 50.0 ± 0.6 for Kap Edward Holm Complex is weighted average of five $^{40}Ar/^{39}Ar$ ages (Nevle *et al.* 1994). *Y*-axis indicates fjord-parallel distance from the mouth of the Kangerlussuaq Fjord at *c.* 68° 01' N and 31° 45' W. Distances have been calculated by projecting intrusion centres onto a NNW–SSE-trending line through the Kangerlussuaq Fjord. Distance to Prinsen af Wales Bjerge Formation lavas is with reference to crater site mapped by Hansen *et al.* (2002). Abbreviations: cc – Cirque 1320 complex; sss – Snout Series Syenite; abc – Astrophyllite Bay Complex; bg – Biotite Granite; KEH – Kap Edward Holm Gabbro Complex.

Iceland mantle plume between 50 and 47 Ma (Bernstein *et al.* 1998; Tegner *et al.* 2008).

6.c. Regional perspective

The chronology of the Kangerlussuaq Fjord lineament has recently been reviewed by Tegner *et al.* (2008). These workers concluded that activity in the fjord was continuous from *c.* 55 to 40 Ma and therefore different from the coastal area further south where magmatic activity was episodic and confined to the time windows 56–54, 50–47 and 37–35 Ma. They note, however, that most of the activity in the Kangerlussuaq Fjord occurred within the time windows quoted above and interpret the post-break-up alkaline intrusions as products of off-axis magmatism in relation to a northwards-propagating mid-ocean ridge, in addition to influences from the Iceland mantle plume. We agree with Tegner *et al.* (2008) that activity in the Kangerlussuaq Fjord was to a large extent continuous. However, in light of the new age constraints discussed in the previous section (see also Fig. 7), it appears that most of the alkaline activity occurred prior to 50 Ma. It is also noteworthy that the oldest pre-50 Ma alkaline rocks are found north of Kærven in the inner parts of the fjord and further inland (Gardiner Complex and Prinsen af Wales Bjerge Formation), but become progressively younger towards the mouth of the fjord (Figs 1, 7). This indicates that the locus of alkaline magmatism migrated in a SSE direction. The post-50 Ma alkaline activity appears to have been more episodic and confined to the outer parts of the fjord and in the coastal region.

To explain this pattern, we propose that the pre-50 Ma alkaline intrusions and lavas record the track of the Iceland hotpot during the rift-to-drift transition. The proposed hotspot track is in accordance with plate-tectonic reconstructions which generally involve passage of the Iceland hotspot through or close to the Kangerlussuaq Fjord (Fig. 1; e.g. Lawver & Müller, 1994; Torsvik *et al.* 2001; Braun *et al.* 2007). It is also consistent with local dome-like uplift in the Kangerlussuaq area around 50 Ma, as proposed by Gleadow and Brooks (1979) on the basis of field evidence and fission-track thermochronology. Assuming that the plume axis reached the coast at *c.* 50 Ma (Bernstein *et al.* 1998; Tegner *et al.* 1998) but was located *c.* 50 km further inland at *c.* 53.5 Ma, as recorded by the Kærven Complex discussed here, leads to an estimated average NW-directed continental drift of *c.* 1.5 cm a^{-1}. This is considerably slower than the 4.4 cm a^{-1} half-spreading rate suggested by Larsen & Saunders (1998) for the initial stages of seafloor spreading; however, it is in agreement with more recent results which indicate that the half-spreading rate dropped from an initial 2.2 cm a^{-1} to

https://doi.org/10.1017/S0016756815000448 Published online by Cambridge University Press

1.5 cm a^{-1} after anomaly 24 (*c.* 53 Ma), before stabilizing at 1.0 cm a^{-1} after anomaly 21 (*c.* 47 Ma) (Smallwood & White, 2002).

Using these rates and assuming that the plume was positioned beneath Kærven at 53.5 Ma, we can backtrack the position of the plume to an area near the Gardiner Complex and the Prinsen af Wales Bjerge Formation at *c.* 56 Ma (Fig. 1). This is consistent with the oldest ages determined for these centres (Fig. 7). On the other hand, at *c.* 47 Ma the plume would have been positioned roughly beneath the continent–ocean boundary (Fig. 1).

The pre-50 Ma alkaline centres of the Kangerlussuaq Fjord likely record low-degree melts produced by upwelling of the mantle plume beneath a relatively thick lithospheric lid, as suggested by Peate *et al.* (2003) for the Prinsen af Wales Bjerge Formation. This process may have been facilitated by thinning of the lithosphere during the rifting attempt recorded by the THOL-2 dykes and the tholeiitic Kærven Gabbro. Conversely, passing of the mantle plume axis beneath thinner lithosphere at the East Greenland rifted margin at 50–47 Ma resulted in greater degrees of melting and a broader melting column. This led to renewed tholeiitic magmatism in the coastal region (e.g. Kap Edward Holm Complex), as well as minor transitional to alkaline activity (TRANS-1 and ALK-1 dykes, and younger satellites of the KAC; Figs 1, 7).

The rifted margin had migrated away from the plume axis at *c.* 47 Ma, resulting in a decline in magmatism. Sporadic alkaline magmatic activity is however recorded in the Kangerlussuaq Fjord between *c.* 45 and 35 Ma by the ALK-2 dykes, the Hutchinson Gletscher Syenite 1 and the Flammefjeld complex (Brooks *et al.* 2004; Tegner *et al.* 2008; Fig. 7). The cause of this final phase of activity is unclear, but we speculate that the northwards propagation of the proto-Reykjanes Ridge/Kolbeinsey Ridge system at *c.* 49–47 Ma may have played a role (Gaina, Gernigon & Ball, 2009). Minor alkaline activity in the Wiedemann Fjord – Kronborg Gletscher lineament north of Kangerlussuaq between *c.* 52 and 36 Ma and the 49–44 Ma tholeiitic–alkaline Kap Dalton Group sequence (Fig. 1) may also have been related to this event (Tegner *et al.* 2008; Larsen *et al.* 2013). Alternatively, this phase was related to a late episode of epeirogenic uplift and erosion culminating at *c.* 35 Ma, as indicated by fission-track thermochronology (Gleadow & Brooks, 1979), possibly in response to plate tectonic reorganization associated with cessation of seafloor spreading in the Labrador Sea (Brooks *et al.* 2004; Tappe *et al.* 2007; Tegner *et al.* 2008).

7. Conclusions

Zircons from six monzonitic, syenitic and granitic intrusive units of the eastern and western parts of the alkaline Kærven Complex have been dated by the U–Pb technique. Zircons from East Kærven units yield concordant and overlapping U–Pb ages, indicating intrusion within a relatively short time span between *c.* 53.5 and 53.3 Ma. Zircons from West Kærven show a greater spread in ages but are generally within range of the East Kærven zircons, indicating that most of the felsic units are of similar age.

The U–Pb ages from East Kærven are younger than the 55.5 ± 1.4 Ma $^{40}Ar/^{39}Ar$ age of Tegner *et al.* (2008) for the tholeiitic Kærven Gabbro, consistent with field evidence indicating that the felsic units largely postdate the gabbro. Minor gabbroic activity may, however, have occurred penecontemporaneously with the felsic intrusions as indicated by the 53.0 ± 0.3 Ma U–Pb age for a gabbro pegmatite by Holm, Heaman & Pedersen (2006).

The U–Pb ages of the Kærven Complex and the Re–Os age of the Cirque 1320 Complex (Holwell *et al.* 2012) constrain the Kangerlussuaq Nordmarkite to have been intruded between *c.* 53.5 and 52.7 Ma, and we infer that most of the KAC was intruded during this time window.

The alkaline intrusions of the Kangerlussuaq Fjord are considered to record the track of the Iceland hotspot during the rift-to-drift transition of the East Greenland rifted margin. Our calculations indicate that the axis of the plume was positioned in the area around the Gardiner Complex and the Prinsen af Wales Bjerge Formation during continental break-up. At *c.* 47 Ma the plume axis was positioned roughly beneath the continent–ocean boundary.

Acknowledgements. LMH acknowledges financial support from NSERC (Discovery and Major Resources Support Grants). J. Schultz is gratefully thanked for assistance in the laboratory and help with mineral picking. G. Hatchard and J. LeBlanc are thanked for help with TIMS analyses at the University of Alberta. Mineral separation was carried out by P. Venslev (University of Copenhagen). The manuscript has benefited from constructive criticism by F. Corfu and an anonymous reviewer, for which we are sincerely grateful.

Supplementary material

To view supplementary material for this article, please visit http://dx.doi.org/10.1017/S0016756815000448.

References

ANDREASEN, R., PEATE, D.W. & BROOKS, C.K. 2004. Magma plumbing systems in large igneous provinces: inferences from cyclical variations in Palaeogene East Greenland basalts. *Contributions to Mineralogy and Petrology* **147**, 438–52.

BECKINSALE, R.B., BROOKS, C.K. & REX, D.C. 1970. K–Ar ages for the Tertiary of East Greenland. *Bulletin of the Geological Society of Denmark* **20**, 27–37.

BERNSTEIN, S., KELEMEN, P.B., TEGNER, C., KURZ, M.D., BLUSZTAJN, J. & BROOKS, C.K. 1998. Post-breakup basaltic magmatism along the East Greenland Tertiary rifted margin. *Earth and Planetary Science Letters* **160**, 845–62.

BRAUN, A., KIM, H.R., CSATHO, B. & VON FRESE, R.R.B. 2007. Gravity-inferred crustal thickness of Greenland. *Earth and Planetary Science Letters* **262**, 138–58.

BROOKS, C.K. 1973. Rifting and doming in southern East Greenland. *Nature* **244**, 23–5.

BROOKS, C.K. 2011. The East Greenland rifted volcanic margin. *Geological Survey of Denmark and Greenland Bulletin* **24**, 1–96.

BROOKS, C.K. & GILL, R.C.O. 1982. Compositional variation in the pyroxenes and amphiboles of the Kangerdlugssuaq intrusion, East Greenland: further evidence for the crustal contamination of syenite magma. *Mineralogical Magazine* **45**, 1–9.

BROOKS, C.K. & PLATT, R.G. 1975. Kaersutite-bearing gabbroic inclusions and the late dike swarm of Kangerdlugssuaq, East Greenland. *Mineralogical Magazine* **40**, 259–83.

BROOKS, C.K., TEGNER, C., STEIN, H. & THOMASSEN, B. 2004. Re–Os and ^{40}Ar–^{39}Ar ages of porphyry molybdenum deposits in the East Greenland volcanic rifted margin. *Economic Geology* **99**, 1215–22.

BURKE, K. & DEWEY, J.F. 1973. Plume-generated triple junctions: key indicators in applying plate tectonics to old rocks. *Journal of Geology* **81**, 406–33.

DEER, W.A. & KEMPE, D.R.C. 1976. Geological investigations in East Greenland: Part XI. The minor peripheral intrusion, Kangerdlugssuaq, East Greenland. *Meddelelser om Grønland* **197**, 1–25.

DUNCAN, R.A. & RICHARDS, M.A. 1991. Hotspots, mantle plumes, flood basalts, and true polar wander. *Reviews of Geophysics* **29**, 31–50.

FROST, B.R. & FROST, C.D. 2008. A geochemical classification for feldspathic igneous rocks. *Journal of Petrology* **49**, 1955–69.

GAINA, C., GERNIGON, L. & BALL, P. 2009. Palaeocene–Recent boundaries in the NE Atlantic and the formation of the Jan Mayen microcontinent. *Journal of the Geological Society of London* **166**, 601–16.

GLEADOW, A.J.W. & BROOKS, C.K. 1979. Fission track dating, thermal histories and tectonics of igneous intrusions in East Greenland. *Contributions to Mineralogy and Petrology* **71**, 45–60.

HAMILTON, E.I. 1966. The isotopic composition of lead in igneous rocks. *Earth and Planetary Science Letters* **1**, 30–7.

HANAN, B.B. & SCHILLING, J.-G. 1997. The dynamic evolution of the Iceland mantle plume: the lead isotope perspective. *Earth and Planetary Science Letters* **151**, 43–60.

HANGHØJ, K., STOREY, M. & STECHER, O. 2003. An isotope and trace element study of the East Greenland Tertiary dyke swarm: constraints on temporal and spatial evolution during continental rifting. *Journal of Petrology* **44**, 2081–2112.

HANSEN, H. & NIELSEN, T.F.D. 1999. Crustal contamination in Palaeogene East Greenland flood basalts: plumbing system evolution during continental rifting. *Chemical Geology* **157**, 89–118.

HANSEN, H., PEDERSEN, A.K., DUNCAN, R.A., BIRD, D.K., BROOKS, C.K., FAWCETT, J.J., GITTINS, J., GORTON, M. & O'DAY, P. 2002. Volcanic stratigraphy of the southern Prinsen af Wales Bjerge region, East Greenland. In *The North Atlantic Igneous Province: Stratigraphy, Tectonic, Volcanic and Magmatic Processes* (eds D.W. Jolley & B.R. Bell), pp. 183–218. Geological Society of London, Special Publication no. 197.

HEAMAN, L.M., BÖHM, CH.O., MACHADO, N., KROGH, T.E., WEBER, W. & CORKERY, M.T. 2011. The Pikwitonei Granulite Domain, Manitoba: a giant Neoarchean high-grade terrane in the northwest Superior Province. *Canadian Journal of Earth Sciences* **48**, 205–45.

HEAMAN, L.M., ERDMER, P. & OWEN, J.V. 2002. U–Pb geochronologic constraints on the crustal evolution of the Long Range Inlier, Newfoundland. *Canadian Journal of Earth Sciences* **39**, 845–65.

HIRSCHMANN, M.M., RENNE, P.R. & MCBIRNEY, A.R. 1997. ^{40}Ar/^{39}Ar dating of the Skaergaard intrusion. *Earth and Planetary Science Letters* **146**, 645–58.

HOLM, P.M. 1991. Radiometric age determinations in the Kærven area, Kangerdlugssuaq, East Greenland Tertiary igneous Province: ^{40}Ar/^{39}Ar, K/Ar and Rb/Sr isotopic results. *Bulletin of the Geological Society of Denmark* **38**, 183–201.

HOLM, P.M., HEAMAN, L.M. & PEDERSEN, L.E. 2006. Baddeleyite and zircon U–Pb ages from the Kærven area, Kangerlussuaq: implications for the timing of Paleogene continental breakup in the North Atlantic. *Lithos* **92**, 238–50.

HOLM, P.M. & PRÆGEL, N.-O. 2006. Cumulates from primitive rift-related East Greenland Paleogene magmas: petrological and isotopic evidence from the ultramafic complexes at Kælvegletscher and near Kærven. *Lithos* **92**, 251–75.

HOLM, P.M., PRÆGEL, N.-O. & EGEBERG, D.G. 1991. Multiple syenite intrusions at Kærven, Kangerdlugssuaq, East Greenland: evidence from the 1986 field work. *Bulletin of the Geological Society of Denmark* **38**, 173–81.

HOLWELL, D.A., SELBY, D., BOYCE, A.J., GILBERTSON, J.A. & ABRAHAM-JAMES, T. 2012. A Re–Os date for molybdenite-bearing quartz vein mineralization within the Kangerlussuaq Alkaline Complex, East Greenland: implications for the timing of regional metallogenesis. *Economic Geology* **107**, 713–22.

IRVINE, T.N. & BARAGAR, W.R.A. 1971. A guide to the chemical classification of the common volcanic rocks. *Canadian Journal of Earth Sciences* **8**, 523–48.

KARSON, J.A. & BROOKS, C.K. 1999. Structural and magmatic segmentation of the Tertiary East Greenland volcanic rifted margin. In *Continental Tectonics* (eds C. MacNiocaill & P.D. Ryan), pp. 313–38. Geological Society of London, Special Publication no. 164.

KEMPE, D.R.C., DEER, W.A. & WAGER, L.R. 1970. Geological investigations in East Greenland. Part VIII. The petrology of the Kangerlussuaq alkaline intrusion. East Greenland. *Meddelelser om Grønland* **190**, 1–49.

KLAUSEN, M.B. & LARSEN, H.C. 2002. East Greenland coast-parallel dike swarm and its role in continental breakup. In *Volcanic Rifted Margins* (eds M.A. Menzies, S.L. Klemperer, C.J. Ebinger & J. Baker) pp. 133–58. Geological Society of America, Boulder, Colorado, Special Paper 362.

KUIPER, K.F., DEINO, A., HILGEN, F.J., KRIJGSMAN, W., RENNE, P.R. & WIJBRANS, J.R. 2008. Synchronizing rock clocks of Earth history. *Science* **320**, 500–4.

LARSEN, H.C. 1990. The East Greenland shelf. In *The Arctic Ocean Region* (ed J.F. Sweeney), pp. 185–210. Geological Society of America, Boulder, Colorado, The Geology of North America volume L.

LARSEN, H.C. & SAUNDERS, A.D. 1998. Tectonism and volcanism at the southeast Greenland rifted margin: a record of plume impact and later continental rupture. In *Proceedings of the Ocean Drilling Program, Scientific Results* (eds A.D. Saunders, H.C. Larsen & S.W. Wise Jr), vol. 152, pp. 503–33. College Station, Texas (Ocean Drilling Program).

LARSEN, L.M., PEDERSEN, A.K., SØRENSEN, E.V., WATT, W.S. & DUNCAN, R.A. 2013. Stratigraphy and age of the Eocene Igtertivâ Formation basalts, alkaline pebbles and sediments of the Kap Dalton Group in the graben at Kap Dalton, East Greenland. *Bulletin of the Geological Society of Denmark* **61**, 1–18.

LARSEN, R.B. & BROOKS, C.K. 1994. Origin and evolution of gabbroic pegmatites in the Skaergaard Intrusion, East Greenland. *Journal of Petrology* **35**, 1651–79.

LAWVER, L.A. & MÜLLER, R.D. 1994. Iceland hotspot track. *Geology* **22**, 311–4.

LE MAITRE, R.W., STREICKEISEN, A., ZANETTIN, B., LE BAS, M.J., BONIN, B., BATEMAN, P., BELLIENI, G., DUDEK, A., EFREMOVA, S., KELLER, J., LAMEYRE, J., SABINE, P.A., SCHMID, R., SØRENSEN, H. & WOOLLEY, A.R. (eds) 2002. *Igneous Rocks: A Classification and Glossary of Terms: Recommendations of the International Union of Geological Sciences Subcommission on the Systematics of Igneous Rocks*. Cambridge: Cambridge University Press, 236 pp.

LENOIR, X., FÉRAUD, G. & GEOFFREY, L. 2003. High-rate flexure of the East Greenland volcanic margin: constraints from $^{40}Ar/^{39}Ar$ dating of basaltic dykes. *Earth and Planetary Science Letters* **213**, 515–28.

LUDWIG, K.R. 2003. Isoplot/Ex 3.00. *A geochronological toolkit for Microsoft Excel*. Berkeley Geochronology Center, Special Publication no. 4, 75 pp.

MCBIRNEY, A.R. 1989. The Skaergaard Layered Series: I. Structure and average compositions. *Journal of Petrology* **30**, 363–99.

MCDOUGALL, I. & HARRISON, T.M. 1988. *Geochronology and thermochronology of the $^{40}Ar/^{39}Ar$ method*. Oxford: Oxford University Press, Oxford Monographs on Geology and Geophysics, 212 pp.

MILLER, J.S., MATZEL, J.E.P., MILLER, C.F., BURGESS, S.D. & MILLER, R.B. 2007. Zircon growth and recycling during the assembly of large composite arc plutons. *Journal of Volcanology and Geothermal Research* **167**, 282–99.

MILLER, J.S. & WOODEN, J.L. 2004. Residence, resorption and recycling of zircons in Devils Kitchen rhyolite, Coso Volcanic Field, California. *Journal of Petrology* **45**, 2155–70.

MIN, K., MUNDIL, R., RENNE, P.R. & LUDWIG, K.R. 2000. A test for systematic errors in $^{40}Ar/^{39}Ar$ geochronology through comparison with U/Pb analysis of a 1.1 Ga rhyolite. *Geochimica et Cosmochimica Acta* **64**, 73–98.

MYERS, J.S. 1980. Structure of the coastal dyke swarm and associated plutonic intrusions of East Greenland. *Earth and Planetary Science Letters* **46**, 407–18.

MYERS, J.S., DAWES, P.R. & NIELSEN, T.F.D. 1988. *Geological map of Greenland 1:500 000, Kangerdlugssuaq, Sheet 13*. Geological Survey of Greenland and Denmark, Copenhagen.

NEVLE, R.J., BRANDRISS, M.E., BIRD, D.K., MCWILIAMS, M.I. & O'NEILL, J.R. 1994. Tertiary plutons monitor climate change in East Greenland. *Geology* **22**, 775–8.

NIELSEN, T.F.D. 1978. Tertiary dike swarms of the Kangerdlugssuaq area, East Greenland. An example of magmatic development during continental break-up. *Contributions to Mineralogy and Petrology* **69**, 235–44.

NIELSEN, T.F.D. 1987. Tertiary alkaline magmatism in East Greenland: a review. In *Alkaline Igneous Rocks* (eds. J.G. Fitton & B.G.J. Upton), pp. 489–515. Geological Society of London, Special Publication no. 30.

PANKHURST, R.J., BECKINSALE, R.D. & BROOKS, C.K. 1976. Strontium and oxygen isotope evidence relating to the petrogenesis of the Kangerdlugssuaq alkaline intrusion, East Greenland. *Contributions to Mineralogy and Petrology* **54**, 17–42.

PEATE, D.W. & STECHER, O. 2003. Pb isotope evidence for contributions from different Iceland mantle components to Palaeogene East Greenland flood basalts. *Lithos* **67**, 39–52.

PEATE, D.W., BAKER, J.A., BLICHERT-TOFT, J., HILTON, D.R., STOREY, M., KENT, A.J.R., BROOKS, C.K., HANSEN, H., PEDERSEN, A.K. & DUNCAN, R.A. 2003. The Prinsen af Wales Bjerge Formation lavas, East Greenland: the transition from tholeiitic to alkalic magmatism during Palaeogene continental break-up. *Journal of Petrology* **44**, 279–304.

PEATE, D.W., BARKER, A.K., RIISHUUS, M.S. & ANDREASEN, R. 2008. Temporal variations in crustal assimilation of magma suites in the East Greenland flood basalt province: Tracking the evolution of magmatic plumbing systems. *Lithos* **102**, 179–97.

RIISHUUS, M.S., PEATE, D.W., TEGNER, C., WILSON, J.R. & BROOKS, C.K. 2008. Petrogenesis of cogenetic silica-oversaturated and -undersaturated syenites by periodic recharge in a crustally contaminated magma chamber: the Kangerlussuaq intrusion, East Greenland. *Journal of Petrology* **49**, 493–522.

RIISHUUS, M.S., PEATE, D.W., TEGNER, C., WILSON, J.R., BROOKS, C.K. & HARRIS, C. 2006. Temporal evolution of a long-lived syenitic centre: the Kangerlussuaq Alkaline Complex, East Greenland. *Lithos* **92**, 276–99.

RIISHUUS, M.S., PEATE, D.W., TEGNER, C., WILSON, J.R., BROOKS, C.K. & WAIGHT, T.E. 2005. Petrogenesis of syenites at a rifted continental margin: origin, contamination and interaction of alkaline mafic and felsic magmas in the Astrophyllite Bay Complex, East Greenland. *Contributions to Mineralogy and Petrology* **149**, 350–71.

SAUNDERS, A.D., FITTON, J.G., KERR, A.C., NORRY, M.J. & KENT, R.W. 1997. The North Atlantic igneous province. In *Large Igneous Provinces: Continental, Oceanic, and Planetary Flood Volcanism* (eds M.F. Coffin & J.J. Mahoney), pp. 45–93. American Geophysical Union, Geophysical Monograph no. 100.

SCHÄRER, U. 1984. The effect of initial ^{230}Th disequilibrium on young U–Pb ages: the Makalu case, Himalaya. *Earth and Planetary Science Letters* **67**, 191–204.

SMALLWOOD, J.R. & WHITE, R.S. 2002. Ridge–plume interaction in the North Atlantic and its influence on continental breakup and seafloor spreading. In *The North Atlantic Igneous Province: Stratigraphy, Tectonic, Volcanic and Magmatic Processes* (eds D.W. Jolley & B.R. Bell), pp. 15–37. Geological Society of London, Special Publication no. 197.

STEIGER, R.H. & JÄGER, E. 1977. Subcomission on geochronology: convention on the use of decay constants in geo- and cosmochronology. *Earth and Planetary Science Letters* **36**, 359–62.

STEIN, H.J., MARKEY, R.J., MORGAN, J.W., HANNAH, J.L. & SCHERSTÉN, A. 2001. The remarkable Re–Os chronometer in molybdenite: how and why it works. *Terra Nova* **13**, 479–86.

STOREY, M., DUNCAN, R.A. & SWISHER III, C.C. 2007. Paleocene-Eocene thermal maximum and the opening of the northeast Atlantic. *Science* **316**, 587–9.

STOREY, M., DUNCAN, R.A. & TEGNER, C. 2007. Timing and duration of volcanism in the North Atlantic Igneous Province: implications for geodynamics and links to the Iceland hotspot. *Chemical Geology* **241**, 264–81.

STRACKE, A., ZINDLER, A., SALTERS, V.J.M., MCKENZIE, D., BLICHERT-TOFT, J., ALBARÈDE, F. & GRÖNVOLD, K.

2003. Theistareykir revisted. *Geochemistry, Geophysics, Geosystems* **4**, doi: 10.1029/2001GC000201.

TAPPE, S., FOLEY, S.F., STRACKE, A., ROMER, R.L., KJARSGAARD, B.A., HEAMAN, L.M. & JOYCE, N. 2007. Craton reactivation on the Labrador Sea margins: $^{40}Ar/^{39}Ar$ age and Sr–Nd–Hf–Pb isotope constraints from alkaline and carbonatite intrusives. *Earth and Planetary Science Letters* **256**, 433–54.

TEGNER, C., BROOKS, C.K., DUNCAN, R.A., HEISTER, L.E. & BERNSTEIN, S. 2008. $^{40}Ar–^{39}Ar$ ages of intrusions in East Greenland: rift-to-drift transition over the Iceland hotspot. *Lithos* **101**, 480–500.

TEGNER, C., DUNCAN, R.A., BERNSTEIN, S., BROOKS, C.K., BIRD, D.K. & STOREY, M. 1998. $^{40}Ar–^{39}Ar$ geochronology of Tertiary mafic intrusions along the East Greenland rifted margin: relation to flood basalts and the Iceland hotspot track. *Earth and Planetary Science Letters* **156**, 75–88.

TODT, M.W., CLIFF, R.A., HANSER, A. & HOFMANN, A.W. 1996. Evaluation of a $^{202}Pb–^{205}Pb$ double spike for high-precision lead isotope analysis. *Geophysical Monograph* **95**, 429–37.

TORSVIK, T.H., MOSAR, J. & EIDE, E.A. 2001. Cretaceous–Tertiary geodynamics: a North Atlantic exercise. *Geophysical Journal International* **146**, 850–66.

WAGER, L.R. 1965. The form and internal structure of the alkaline Kangerdlugssuaq intrusion, East Greenland. *Mineralogical Magazine* **34**, 487–97.

WAIGHT, T., BAKER, J. & WILLIGERS, B. 2002. Rb isotope dilution analyses by MC-ICPMS using Zr to correct for mass fractionation: towards improved Rb–Sr geochronology? *Chemical Geology* **186**, 99–116.

WHITE, R. & MCKENZIE, D. 1989. Magmatism at rift zones. The generation of volcanic continental margins and flood basalts. *Journal of Geophysical Research* **94**, 7685–729.

WOTZLAW, J.-F., BINDEMAN, I.N., SCHALTEGGER, U., BROOKS, C.K. & NASLUND, H.R. 2012. High-resolution insights into episodes of crystallization, hydrothermal alteration and remelting in the Skaergaard intrusive complex. *Earth and Planetary Science Letters* **355–356**, 199–212.